Desalination and Water Treatment
www.deswater.com

doi: 10.1080/19443994.2016.1175384

57 (2016) 26976–26992
December

Taylor & Francis
Taylor & Francis Group

Reducing fouling of polyethersulfone microfiltration membranes by corona air plasma

Samaneh Afkham, Ahmadreza Raisi*, Abdolreza Aroujalian

Department of Chemical Engineering, Amirkabir University of Technology (Tehran Polytechnic), Hafez Ave., P.O. Box 15875-4413, Tehran, Iran, Tel. +98 21 64543290; email: safkham@aut.ac.ir (S. Afkham), Tel. +98 21 64543125; Fax: +98 21 66405847; email: raisia@aut.ac.ir (A. Raisi), Tel. +98 21 64543163; email: aroujali@aut.ac.ir (A. Aroujalian)

Received 5 November 2015; Accepted 22 March 2016

ABSTRACT

In this study, the surface of polyethersulfone (PES) microfiltration membranes was modified by corona discharge plasma in order to improve the antifouling properties and separation performance of the membranes. For this purpose, the PES microfiltration membranes were fabricated by the vapor-induced phase inversion coupled with the nonsolvent-induced phase inversion technique. The effect of the corona power and exposure time on the surface properties and separation performance of the membranes for microfiltration of skim milk was studied. The analysis of the filtration transport resistances was also performed to evaluate the antifouling performance of the corona-modified membranes. The results indicated that the exposure time and applied power of the corona treatment had effects on the membrane surface modification as the surface hydrophilicity, wettability, and morphology of the membranes were significantly changed depending on the corona modification conditions. Moreover, the analysis of the transport resistances revealed that the cake resistance was the main resistance to transport and the fouling, cake and total filtration resistances for the corona-modified PES membranes were low in comparison to the neat PES membranes, which implies that the fouling tendency of the PES membranes modified by the corona air plasma was considerably reduced.

Keywords: Surface modification; Corona treatment; Polyethersulfone (PES) membrane; Microfiltration (MF); Transport resistances

1. Introduction

Microfiltration (MF) is a low pressure-driven membrane separation process which has found wide applications in water and wastewater treatment, petroleum refining, sterilization, fruit juice clarification, dairy processing as well as the production of paints and adhesives [1]. Compared to traditional separation processes, the MF process has significant advantages such as low energy consumption, without the addition of chemicals, no heat damage to heat-sensitive constituents, better removal of contaminants, easy to operate, and well-arranged process conductions. Due to these benefits, the MF has become an important separation process in recent years [2]. However, membrane fouling and flux decline are the main drawback of the MF process in various applications. The membrane fouling is a result of interactions between the membrane and the components present in the feed stream.

*Corresponding author.

Therefore, the membrane surface characteristics such as hydrophilicity, wettability, charge, roughness, and porosity which determine the interactions between the membrane and feed solution, strongly affect the fouling. Depending on the chemical nature of foulants, the fouling is classified into four categories: inorganic fouling or scaling, organic fouling, colloidal fouling, and biological fouling or biofouling [3]. The membrane fouling leads to a decrease in the membrane flux, deterioration of the membrane structure, and an increase in energy and membrane replacement costs [4]. Therefore, it is necessary to employ a technique to reduce the fouling phenomena. Various methods including membrane cleaning, feed pretreatment, optimization of operating conditions and changing the flow regimes, design of new membrane modules, using back-pulsing, back-flushing and back-washing techniques, use of antiscalant materials and membrane modification were applied to reduce the membrane fouling [4–7].

In recent years, several attempts have been made to develop membranes with antifouling properties via modification of the membrane. Generally, both hydrophilic and hydrophobic polymeric materials have been employed to prepare the membrane for use in the microfiltration process. Most commercial MF membranes are made from the hydrophobic polymers like polyethersulfone (PES), polysulfone (PSf), polyvinylidenefluoride (PVDF), polytetrafluoroethene (PTFE), and polypropylene (PP), due to their superior excellent mechanical and thermal properties as well as outstanding chemical resistance. However, the hydrophilic membranes are less susceptible to fouling than the hydrophobic ones [8]. Thus, the main objective of the membrane modification is to combine the surface chemistry of the hydrophilic materials with excellent bulk properties of the hydrophobic polymers. The membrane modification can be achieved by amendment of the membrane matrix or modification of the membrane surface. Techniques such as blending with hydrophilic and amphiphilic polymers [9] and the addition of inorganic materials [10] have been applied to modify the membrane matrix. On the other hand, the surface modification has the advantages of ameliorating the surface properties like wettability, hydrophilicity, and polarity without serious changes on the membrane bulk properties [11]. The membrane surface can be modified via surface coating [12], grafting of hydrophilic monomers [13,14], covalent attachment hydrophilic polymers [15,16], irradiation [17,18], and cold plasma treatment [19–39].

The cold plasma treatment has been extensively used in various modes including plasma-graft polymerization [19–21], polymerizable vapor plasma [22], and nonpolymerizable gas plasma [23–39] for surface modification of the membranes. Moreover, various cold plasma techniques such as radio frequency (RF) [23–30], glow discharge [31,32], microwave [33,34], and corona discharge [35–39] have been employed to improve the surface properties, fouling resistance, and separation performance of different membranes. Various gases and vapors like air [25,31,37–39], oxygen [23,24,28,30,35,36], carbon dioxide [27], ammonia [26,33], carbon tetrafluoride [32,34], methane [29], argon [23,29], and steam [23] have been applied to modify various microfiltration, ultrafiltration (UF), nanofiltration (NF), and gas separation (GS) membranes. For example, Kim et al. [24] reported that the air and oxygen plasma treatments of the PSf UF membrane enhanced the hydrophilicity of membranes and led to less fouling in the gelatin solutions. Kim et al. [26] found that the RF ammonia plasma treatment of the Commercial nanofiltration (NF) thin-film composite (TFC) membranes decreased the fouling tendency of the modified membranes and improved their filtration performance in the Aldrich humic acid solutions. He et al. [27] showed that RF CO_2 plasma modification of the PP UF membranes efficiently improved the separation performance of the modified membranes for the BSA solutions. Sadeghi et al. [37] evaluated the effects of the corona treatment time and power on the surface modification of PES UF membranes to reduce the membrane fouling and improve the membrane separation performance. Moghimifar et al. [38] applied the corona air plasma to prepare TiO_2 nanoparticles-coated PES UF membranes with antifouling properties for the oily wastewater treatment. Juang et al. [29] modified the surface of the PVDF UF membranes using RF argon plasma and observed that the permeation flux was significantly enhanced with the cyclonic atmospheric pressure plasma. However, Tyzsler et al. [36] observed that the corona oxygen plasma improved the hydrophilicity of the PES UF, but resulted in more fouling of the modified membrane in a long-term membrane bioreactor.

The corona plasma treatment has advantages like continuous operation, environmental compatibility, effectiveness, uniform treatment, simplicity of operation at ambient temperature and pressure [40]. A search in the works on the membrane modification by plasma treatment reveals that the conditions of this process, especially the type of gas as well as the plasma power and exposure time have a significant influence on the surface characteristics and separation performance of the modified membranes. Therefore, it is necessary to study the influence of the plasma treatment on the membrane properties and performance. The main goal of this work is to employ the corona

air plasma in order to modify the polyethersulfone microfiltration membranes and to evaluate the influence of the corona power and exposure time on the membrane surface and bulk properties as well as on the fouling tendency and separation performance of the membranes. For this purpose, the PES microfiltration membranes were prepared by the vapor-induced phase inversion followed by the nonsolvent-induced phase inversion technique and the membrane surface was modified by the corona air plasma at different treatment times and input powers. The antifouling property and separation performance of the modified membrane were investigated by the permeation test of pure water and skim milk. The main innovative aspect of this study is the use of corona air plasma to modify the PES microfiltration membranes for the pasteurization of milk. Another important contribution is the investigation of the effect of corona treatment conditions such as corona power and time on the surface modification and separation performance of the prepared PES membranes.

2. Materials and methods

2.1. Materials

The commercial PES with a molecular weight of 58,000 g/mol (E 6020 P) as membrane material was purchased from BASF (Ludwigshafen, Germany). Triethyleneglycol (TEG) as nonsolvent and N-methyl-2pyrrolidone (NMP) as solvent were supplied from Merck Co. Ltd (Darmstadt, Germany). Potassium oxalate and formaldehyde with high purity utilized for the protein measurement were supplied from Merck Co. Ltd (Darmstadt, Germany). Also, Muller Hinton agar used in the microbial tests was purchased from Merck Co. Ltd (Darmstadt, Germany). Skim milk for the microfiltration experiments was supplied from Mimas Dairy Co. (Tehran, Iran). The composition of the used skim milk is 1% milk fat, 9% solids-not-fat including protein, lactose, minerals, enzymes and vitamins, and 90% water.

2.2. Preparation of PES membrane

The PES microfiltration membranes were fabricated by the vapor-induced phase inversion coupled with the nonsolvent-induced phase inversion technique according to the procedure described by Susanto et al. [41]. In this procedure, the PES polymer was dried in an oven at 100˚C for 4 h. Then, the casting solution was prepared by dissolving 10 g of PES in a mixture of solvent and nonsolvent additive containing 40 g of NMP and 50 g of TEG. The polymer solution was stirred continuously over night to obtain a clear homogenous solution. The obtained solution was de-aerated by a vacuum pump (Busch Inc., Switzerland) for 2 h to obtain a bubble-free polymer solution, and then cast on a glass plate with a steel casting knife. The glass plate was subjected to the humid air with relative humidity of 65–75% for 1 min and then immersed into a nonsolvent bath containing de-ionized water at 50˚C to complete the participation. After coagulation, the formed PES membrane was separated from the glass plate. The prepared membranes were stored in a soaking bath containing de-ionized water for 24 h in order to remove the residual solvent, completely. The membranes were dried at room temperature and the final thickness of the membranes was 80 ± 5 μm.

2.3. Membrane surface modification

In order to modify the prepared PES membranes, the corona air plasma was applied using a commercial device (Naaj Corona, Naaj Plastic Co., Tehran, Iran) at atmospheric pressure according to the procedure previously presented by Moghimifar et al. [38]. A photograph of the corona apparatus is shown in Fig. 1. The membrane samples with size of a 7 × 9 cm were placed on the backing roller covered with the silicon coating and rotating at a given speed. The distance between the backing roller and the aluminum electrode was adjusted to a specific value. The corona plasma was generated within the air gap between the electrode and backing roller. The membrane was treated when the generated corona came into contact with the membrane surface. The corona treatment was performed at various input powers (300, 500, and 700 W) for different time durations (7, 10, and 13 min). The nomenclature of the prepared membranes is presented in Table 1.

2.4. MF experiments

In order to evaluate the separation performance of the neat and corona-treated membranes, the microfiltration experiments were conducted using a flat sheet membrane module in cross-flow mode. The filtration apparatus has been previously described in Toroghi et al. [42]. Fig. 2 shows a schematic of the experimental microfiltration setup. The MF experiments were performed with the pure water and skim milk as feed stream at room temperature and an operating pressure of 1.5 bar. Before the milk microfiltration process, the membrane setup was sterilized by a cleaning in place

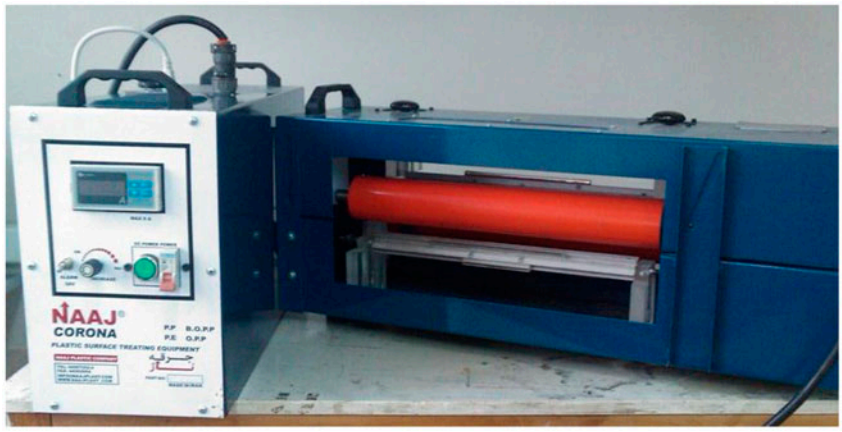

Fig. 1. A photograph of the corona apparatus.

Table 1
The nomenclature of the prepared membranes

Membrane sample	Corona input power (w)	Corona time (min)
M1	–	–
M2	300	7
M3	300	10
M4	300	13
M5	500	7
M6	500	10
M7	500	13
M8	700	7
M9	700	10
M10	700	13

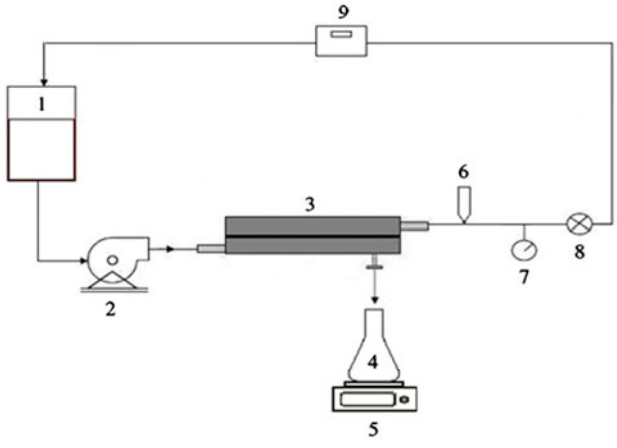

Fig. 2. A schematic of the experimental microfiltration setup.
Notes: (1) feed tank, (2) feed pump, (3) membrane module, (4) permeate, (5) digital balance, (6) pressure controller, (7) pressure gage, (8) valve, and (9) flow meter.

method. Each membrane sample was used in the MF experiments right after the corona modification. The membrane performance was evaluated in terms of mass permeation flux, protein permeability as well as microbial load of the permeate and retentate streams. The pure water and milk permeation flux (J) was calculated by the following equation:

$$J = \frac{w}{At} \tag{1}$$

where w is weight of the collected permeate (kg), A is the membrane area (3.5×10^{-3} m^2), and t is the permeation time (h).

The protein permeability (P_p) of the membranes was determined by measuring the protein content of the feed and permeate streams and calculated as follows:

$$P_p = \frac{C_P}{C_F} \times 100 \tag{2}$$

where C_F and C_P are the protein concentration in the feed and permeate streams, respectively. The Formol titration method was used to determine the protein concentration [43]. In the first step, 10 ml of the milk sample with 1 ml of saturated potassium oxalate solution and phenolphthalein as detector was titrated by 0.1 M sodium hydroxide solution until the mixture color became pink. In the second step, 2 ml formaldehyde was added, and after 2 min, it was titrated again by 0.1 M sodium hydroxide until the appearance of a pink color. All the steps were repeated by 10 ml of the control sample. The protein concentration was calculated as follows:

$$\text{Protein } (\%) = 1.74(V_2 - V_1) \tag{3}$$

where V_1 and V_2 are the volume of consumed sodium hydroxide at the second step for the control and milk sample, respectively.

The colony count method was used to determine the microbial load of the feed, permeate, and retentate streams after 2 h filtration. In this method, samples from the raw milk and permeate and retentate streams were diluted by saline solution (0.9 wt% NaCl aqueous solution) with proper ratio and spread uniformly on the Muller Hinton solid agar. The plates were incubated at 37˚C for 72 h, and then colonies formed on the nutrient agar were counted. The concentration of microbial cells in the samples was obtained after multiplying the number of colonies by the dilution. The neat PES membrane was used as the control sample. The microbe rejection (R) of the prepared MF membrane was determined as follows:

$$R\ (\%) = \left(1 - \frac{N_P}{N_F}\right) \times 100 \tag{4}$$

where N_F and N_P are the microbial content of the feed and permeate streams, respectively.

For each corona treatment condition, at least two or three membrane samples were modified and tested in the MF experiments.

2.5. Fouling analysis

The membrane fouling during the membrane processes including microfiltration leads to the flux decline because fouling increases the resistance against mass transport through the membrane. Therefore, the membrane fouling can be quantified by the resistance appearing during the filtration [44]. The mass flux through a fouled membrane can be expressed as a ratio of the driving force over the total mass transport resistance as follows:

$$J = \frac{\rho}{\mu}\frac{\Delta P}{R_t} \tag{5}$$

where ρ and μ are the fluid density and viscosity, respectively, ΔP is the pressure difference across the membrane and R_t is total mass transport resistance which is the sum of intrinsic membrane resistance (R_m), fouling resistance (R_f), and cake resistance (R_c):

$$R_t = R_m + R_f + R_c \tag{6}$$

$$R_m = \frac{\rho}{\mu}\frac{\Delta P}{J_{wi}} \tag{7}$$

$$R_f = \frac{\rho}{\mu}\frac{\Delta P}{J_{ww}} - R_m \tag{8}$$

$$R_c = \frac{\rho}{\mu}\frac{\Delta P}{J_m} - R_m - R_f \tag{9}$$

where J_{wi} and J_{ww} are the pure water flux of the virgin and fouled membranes, respectively, and J_m is the final steady state milk flux.

Furthermore, the flux recovery ratio (FRR) was calculated to evaluate the antifouling property of the corona-modified membranes, as follows:

$$\text{FRR } (\%) = \frac{J_{ww}}{J_{wi}} \times 100 \tag{10}$$

2.6. Characterization tests

2.6.1. FTIR-ATR spectroscopy

Fourier transmission infrared-attenuated total reflection (FTIR-ATR) spectroscopy was employed to determine the chemical effect of the corona treatment and to characterize the functional groups on the membranes surface. The FTIR-ATR analysis was performed using a Nicolet Nexus 670 spectrometer (Nicolet Instrument Co., Madison, WI, USA) with 4 cm^{-1} resolution over a wave number range of 190–700 cm^{-1} and a 1 × 4 cm sample without further treatment was used for each test. For the corona-modified membranes, the analysis was done right after the sample was exposed to the corona.

2.6.2. Contact angle analysis

The contact angle analysis was utilized to evaluate the changes in the hydrophilicity of the PES membranes after the corona modification. The water contact angle was measured by an optical contact angle instrument (OCA-20; Data Physics GmbH, Filderstadt, Germany) at room temperature with de-ionized water. The contact angle of five different locations on the membrane surface was measured and the average value was recorded.

2.6.3. AFM analysis

Atomic force microscopy (AFM) analysis was used to specify the changes in the surface roughness of the membranes after the corona treatment. The AFM analysis was done by a microscope (NanoEducator, NTMDT Co., Zelenograd, Russia) that was calibrated by the standard samples (TGG1 and TGX1, NT-MDT Co., Zelenograd, Russia) and a 8×8 μm area was scanned by semi-contact mode in the air for each membrane sample. Three different locations of each sample were analyzed and the average values of roughness were reported. The roughness was expressed as average roughness (RA) and root mean square (RMS) values.

2.6.4. SEM analysis

Scanning electron microscopy (SEM) test was applied to determine the morphology of the neat PES membrane and the corona-treated membranes. The SEM analysis was performed using a Hitachi SEM (model S-4160, Hitachi, NJ, USA). The membrane samples were stuck on a holder and coated with a thin layer of gold by sputtering before the analysis.

2.6.5. Membrane pore size and porosity

The filtration velocity method using the Guerout–Elford–Ferry equation was used to estimate the mean pore diameter (D_p) of the PES membranes [45]:

$$D_p = \sqrt{\frac{32(2.9 - 1.75\varepsilon)\eta \ell Q}{\varepsilon A \Delta P}} \tag{11}$$

where ε is the membrane porosity, η is the water viscosity (8.9×10^{-4} Pa s), ℓ is the membrane thickness (m), Q is the volumetric flow rate (m^3/s) of the pure water permeation test, A is the membrane effective area (m^2), and ΔP is the operating pressure (MPa).

The membrane porosity was determined by the water content test as the weight difference between the dried and wet membranes. For this purpose, a dry membrane sample with a definite size was immersed in the de-ionized water bath for 24 h. The soaked membrane was picked up from the bath and water on the surface of the membranes was carefully cleaned with a clean tissue and the membrane was weighed and set down as the membrane weight in the wet state (W_w). Then, the membrane was dried in an oven until the constant weight was obtained and weighed again to measure the membrane weight in dry state (W_d). The membrane porosity was calculated as follows:

$$\varepsilon = \frac{W_w - W_d}{\rho_w V} \tag{12}$$

where ρ_w is the water density and V is the volume of the wet membrane.

3. Results and discussion

3.1. Membrane morphology

A particular change in the hydrophilicity and polarity of the membrane surface after the modification of the PES MF membrane by the corona treatment can be attributed to the changes in the functional groups on the membrane surface. The FTIR-ATR spectroscopy was used to analyze the changes in the chemical structure of the membrane surface and the FTIR-ATR absorbance spectra of the corona-modified

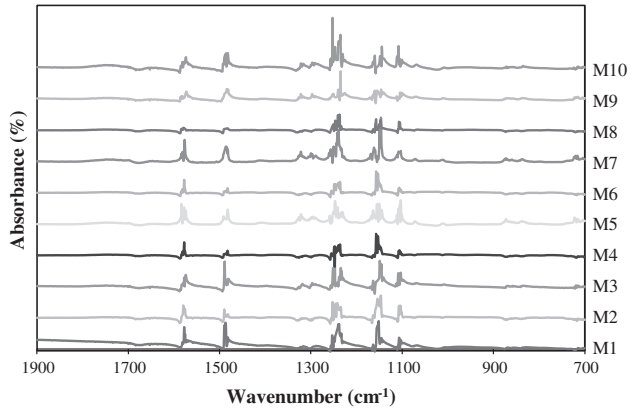

Fig. 3. The FTIR-ATR spectra of the neat and corona-treated PES membranes.

Table 2
The absorbance intensity of the detected functional groups in the FTIR-ATR spectra of various membranes

Membrane	C–O (1,100 cm^{-1})	S=O (1,150 cm^{-1})	C–O–C (1,240 cm^{-1})	C=C (1,480 cm^{-1})	C=C (1,580 cm^{-1})	C–N (1,609 cm^{-1})	C=O (1,660 cm^{-1})
M1	0.0324	0.0507	0.0919	0.2011	0.2009	0.0000	0.0000
M2	0.0413	0.1231	0.1032	0.0239	0.0945	0.0025	0.0011
M3	0.0892	0.1611	0.1212	0.1302	0.0783	0.0091	0.0046
M4	0.0554	0.0668	0.1025	0.0135	0.0169	0.0043	0.0035
M5	0.1244	0.1503	0.1083	0.0933	0.1015	0.0005	0.0007
M6	0.0331	0.1372	0.0719	0.0282	0.0481	0.0091	0.0025
M7	0.0685	0.2232	0.2055	0.0923	0.0604	0.0046	0.0035
M8	0.0402	0.1088	0.0709	0.0393	0.0792	0.0055	0.0014
M9	0.0423	0.0610	0.1047	0.0617	0.0481	0.0017	0.0011
M10	0.0665	0.0727	0.1636	0.0732	0.0680	0.0009	0.0013

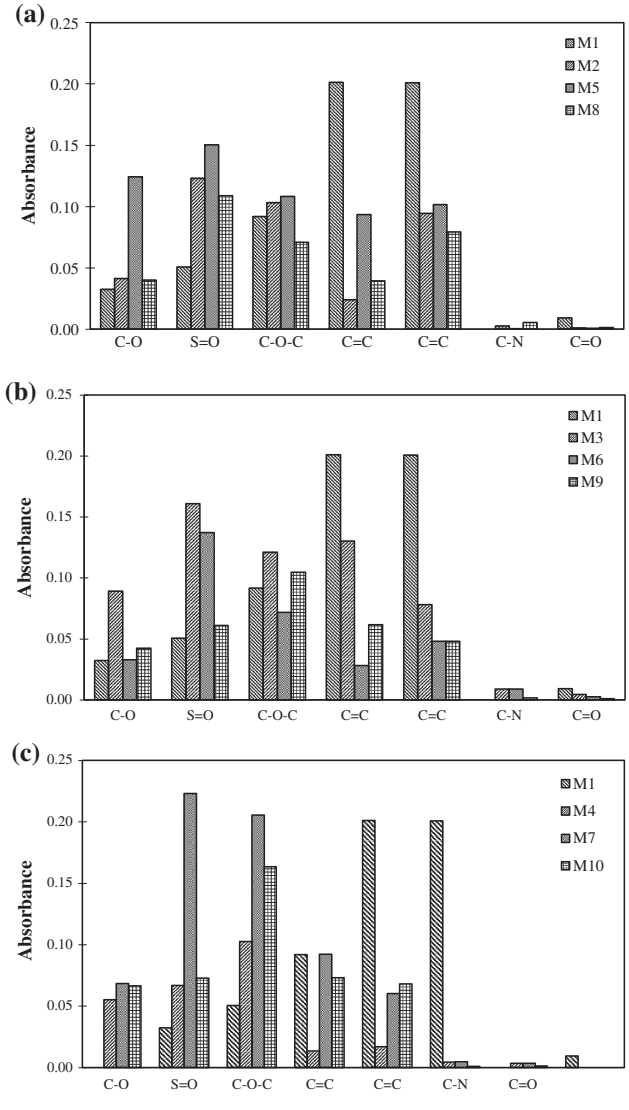

Fig. 4. The effect of corona power on the functional groups of the PES membrane at different exposure times: (a) 7 min, (b) 10 min, and (c) 13 min.

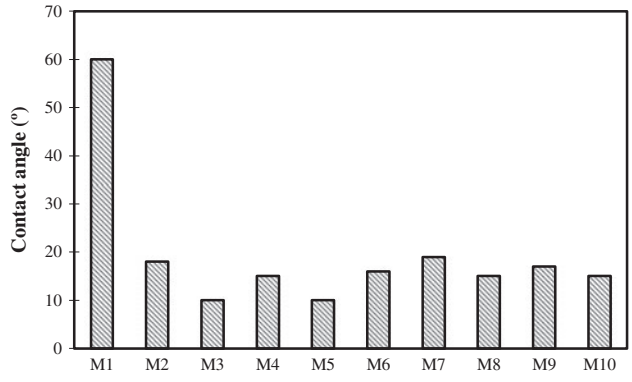

Fig. 5. The water contact angle of the neat and corona-modified membranes.

and neat PES membranes are presented in Fig. 3. In these FTIR-ATR spectra, the absorbance peaks at wave numbers of 1,100, 1,240, 1,150, 1,320, 1,480, and 1,580 cm^{-1} can be attributed to the C–O, C–O–C, asymmetric, and symmetric stretches of S=O and aromatic C=C asymmetric stretching vibration bonds of the PES membrane. Also, the peak of the C–N and C=O groups detected at wave number of 1,609 and 1,660 cm^{-1}, respectively, does not appear in the spectra of the neat PES membrane. In the corona air plasma, the high voltage that is applied between the electrodes ionizes the nitrogen and oxygen molecules in the air gap between the electrodes and generates the ionized compounds and radicals. These charged species attack the surface of the PES membrane and result in the scission of bonds like C=C and formation of polar functional groups such as C=O, C–O and C–N.

The absorbance values of the functional groups for various membranes are given in Table 2. A comparison between the neat and corona-modified PES

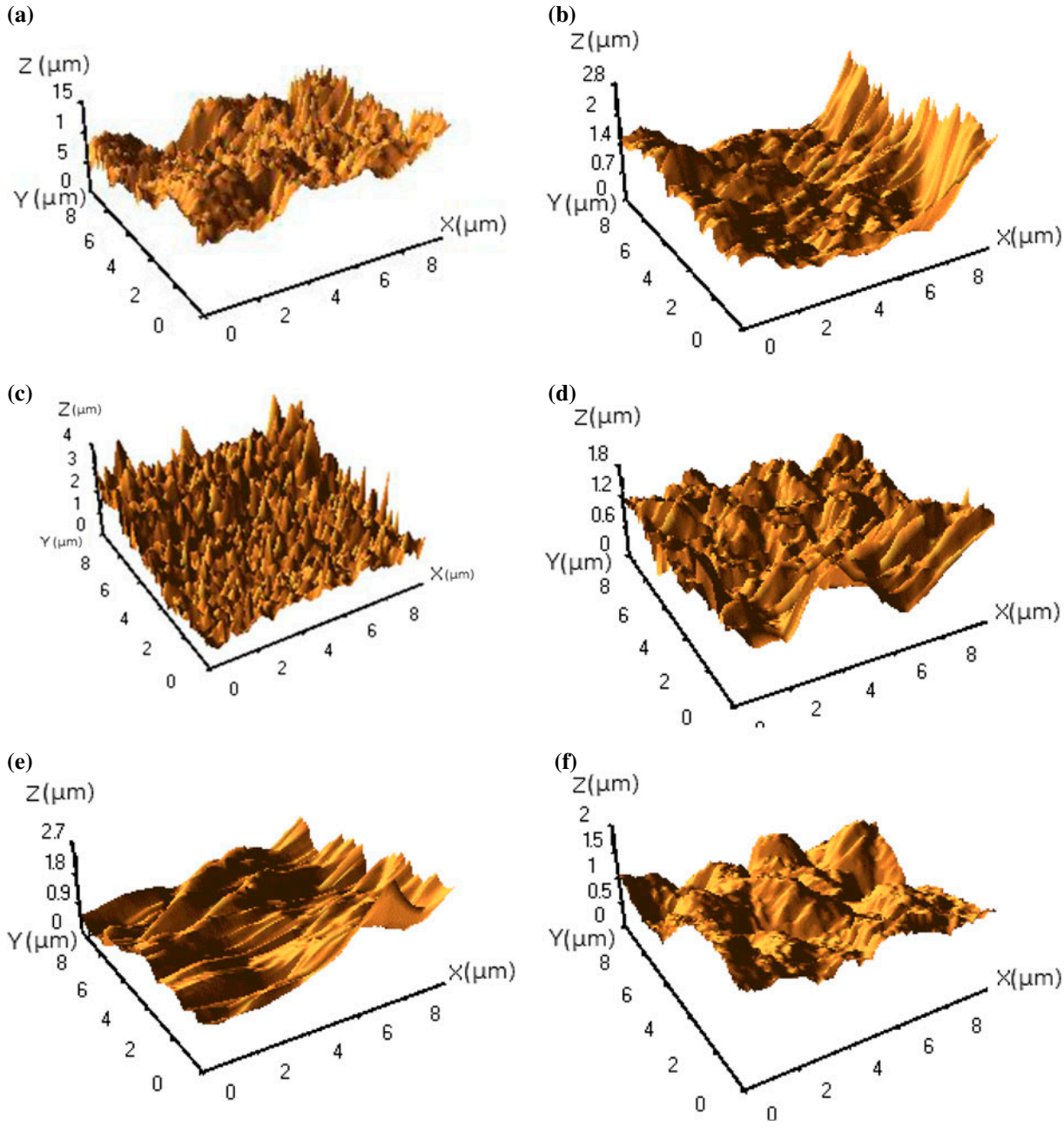

Fig. 6. The AFM images of the neat and corona-modified membranes: (a) M1, (b) M2, (c) M3, (d) M4, (e) M5, (f) M6, (g) M7, (h) M8, (i) M9, and (j) M10.

membranes indicates that the absorbance of some functional groups including the C–O, C–O–C and S=O groups enhances after the corona treatment of the membranes. However, the absorbance intensity of the carbonyl and carbon–carbon double bonds of the corona-treated membrane is lower than those of the neat PES membrane. Also, the effect of corona treatment power and exposure time on the surface modification and functional group changes is shown in Fig. 4. It can be seen that the required time for the functional groups build-up decreases as the corona power increases. During the corona treatment, the plasma, which is a partially ionized gas consisting of large concentrations of excited atomic, molecular, ionic, and free-radical species, is generated and the surface of membrane is bombarded with these excited species.

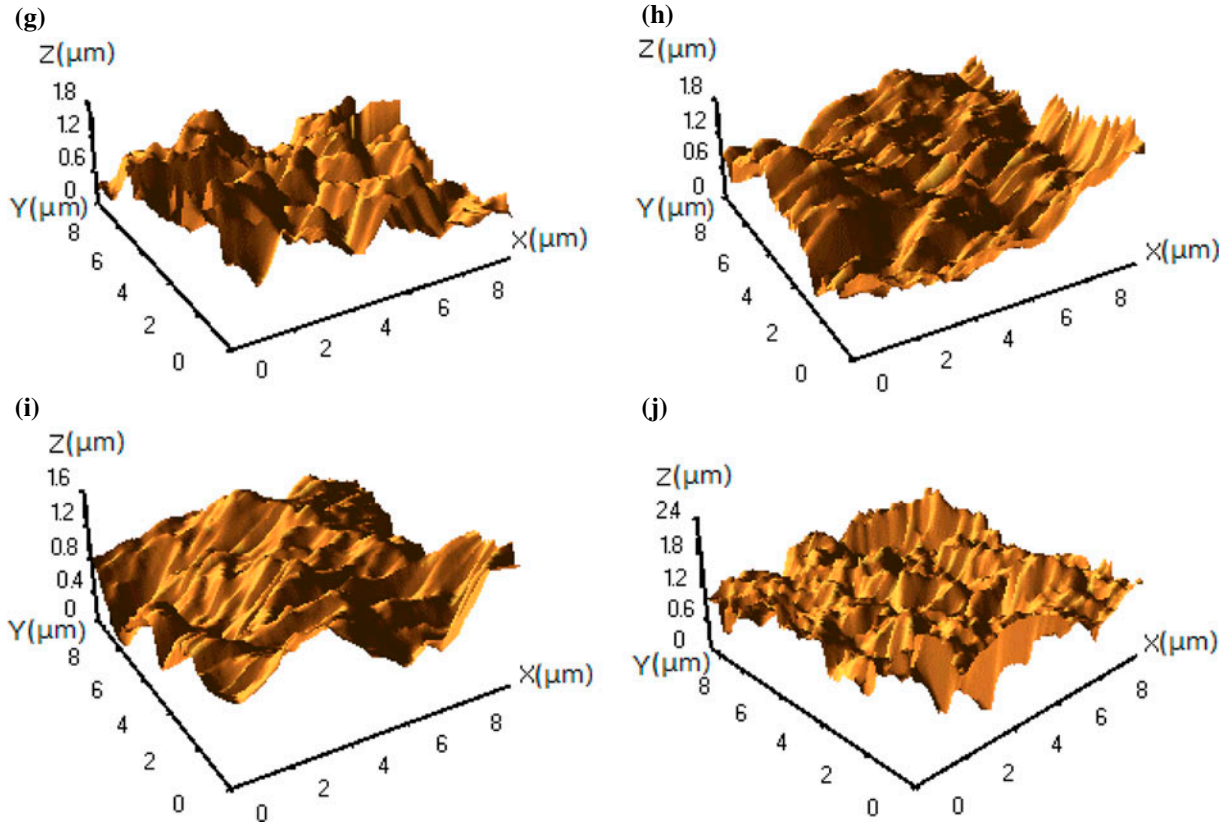

Fig. 6. (*Continued*).

Table 3
The roughness parameters of various PES membranes

Membrane	R_a (nm)	RMS (nm)
M1	507 ± 11	625 ± 9
M2	397 ± 9	445 ± 11
M3	440 ± 7	509 ± 12
M4	343 ± 10	383 ± 13
M5	281 ± 12	330 ± 15
M6	321 ± 8	405 ± 10
M7	403 ± 10	467 ± 11
M8	234 ± 11	306 ± 8
M9	189 ± 13	250 ± 10
M10	277 ± 9	300 ± 11

The interaction of the plasma with the membrane surfaces results in the chemical and physical modification of the membrane surface. The resulting surface changes depend on the composition of the surface, the gas used, and the conditions of the corona treatment. The building and damaging phenomena may occur during the surface modification by the corona plasma treatment. These possible phenomena may counteract one another or overtake the other; therefore, depending on the power and time of the corona treatment, different effects can be seen at different stages [37–39]. As shown in Fig. 4(a), at an input power of 300 W and exposure time of 7 min, the absorbance value of all functional groups except the C=C bond was increased in comparison to the neat PES membrane, although the enhancement in the absorbance value was very low. As the input power increased from 300 to 500 W, the absorbance value of the formed functional groups reached its maximum. A further increase in the corona power led to a decrease in the formation of the functional group because the damaging effect of the corona dominates the building effect. Moreover, a comparison between the FTIR-ATR spectra of the M1, M2, M3, and M4 membrane samples reveals the effect of the corona exposure time on the chemical structure of the PES membranes after the modification by the corona air plasma. For the corona modification at 300 W, the scission of the C=C bond was introduced and the formation of the functional groups increased with an enhancement in the corona exposure time from 7 to 10 min, while a continuous reduction in all

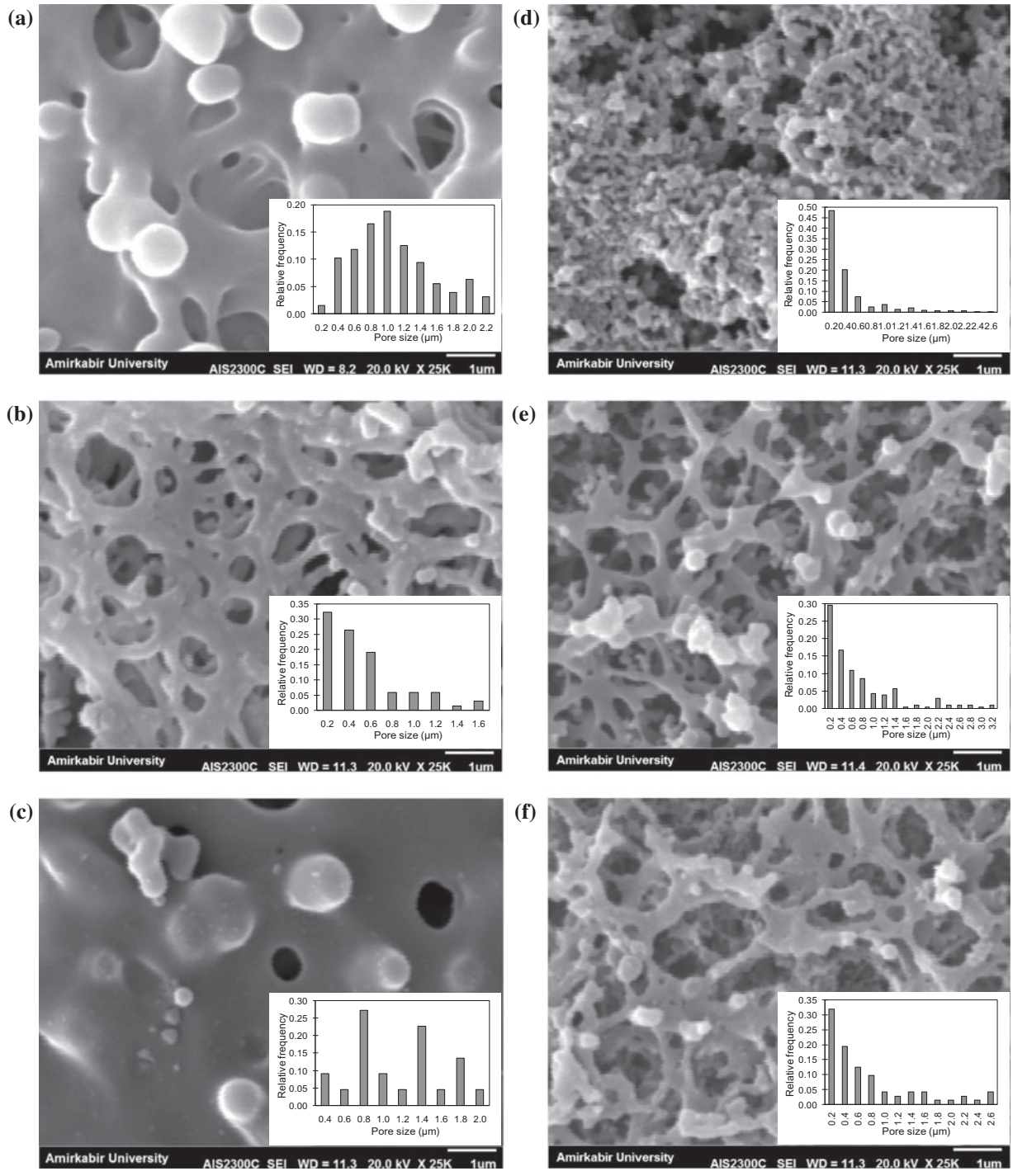

Fig. 7. The SEM images from the surface of the neat and corona-modified membranes: (a) M1, (b) M2, (c) M3, (d) M4, (e) M6, and (f) M9.

functional groups was observed at corona exposure times higher than 10 min. This trend can be related to the damaging effect and deposition of etched materials on the membrane surface which led to a decrease in the absorbance intensity of the functional groups. Generally, it was found that the formation of

Table 4
The porosity and average pore size of the neat membrane and corona-treated PES membranes

Membrane	Average pore size (nm)	Porosity
M1	302 ± 14	0.87 ± 0.21
M2	280 ± 10	0.87 ± 0.23
M3	342 ± 15	0.87 ± 0.15
M4	250 ± 14	0.86 ± 0.12
M5	240 ± 11	0.87 ± 0.18
M6	210 ± 16	0.88 ± 0.22
M7	272 ± 12	0.86 ± 0.26
M8	310 ± 13	0.87 ± 0.19
M9	214 ± 15	0.90 ± 0.22
M10	300 ± 17	0.87 ± 0.26

the functional groups and subsequent degradation effect as well as the deposition of etched materials started faster as the corona input power enhanced.

The contact angle analysis was also used to identify the variation in the hydrophilicity of the PES membranes after the modification by the corona air plasma. Fig. 5 indicated the values of water contact angle of different membranes. It was found that the contact angle of all corona-modified PES membranes was lower than that of the neat membrane. The water contact angle of the neat PES membrane reduces from 60° to 10° for the corona-modified membranes. This reveals that the hydrophilicity of the membrane surface enhances by the corona air plasma treatment. The contact angle results are in good agreement with the FTIR-ATR data. Based on the FTIR-ATR analysis (Fig. 4), the M5 and M3 membrane samples had the highest absorbance intensity of polar functional groups on the membrane surface and the lowest water contact angles were observed for these two membrane samples, as given in Fig. 5.

The changes in the roughness and topography of the membrane surface after modification by the corona treatment were identified by the AFM analysis. The three-dimensional topographic AFM images of various membranes are shown in Fig. 6 and the RMS and RA values are also presented in Table 3. It can be seen that the changes in the surface roughness of the PES membranes with the corona exposure time are different at various corona powers. The physical effects of the corona treatment including the ablation and etching effect as well as the deposition of the etched materials on the membrane surface determine the surface roughness of the membrane after the corona modification. Dominance of one of these two phenomena specifies the changes in the roughness of the membrane

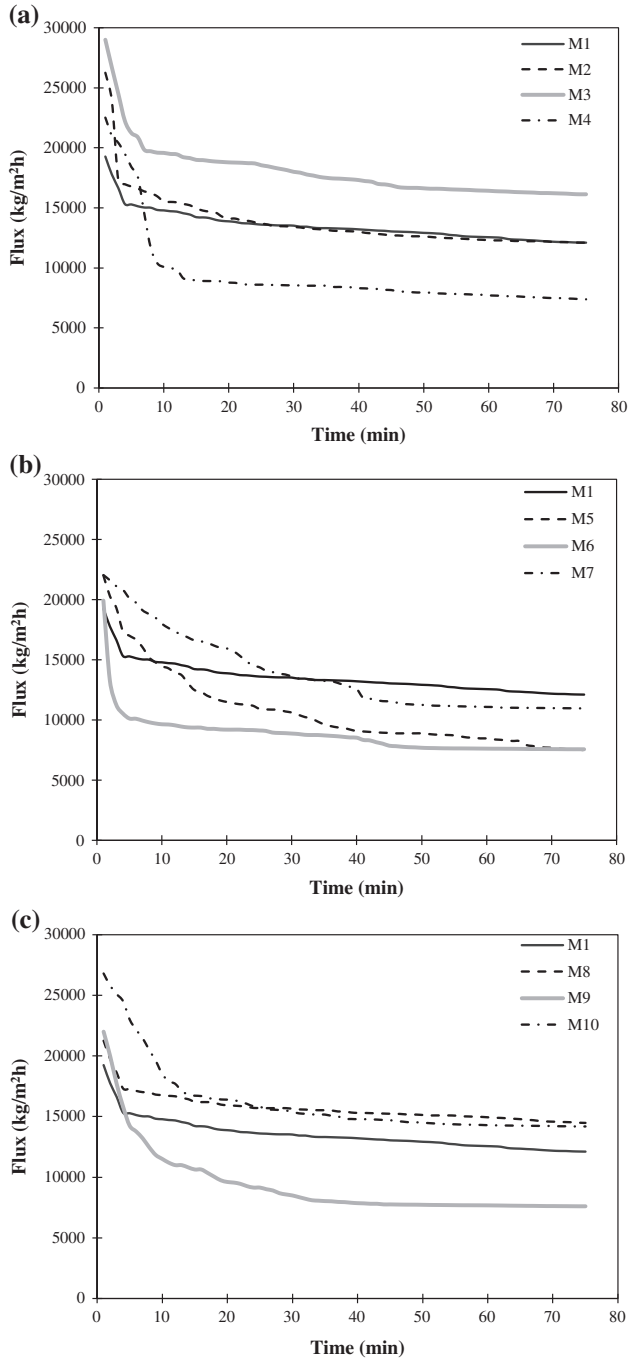

Fig. 8. The pure water flux of the neat PES membrane and corona-modified membranes at different corona powers: (a) 300 W, (b) 500 W, and (c) 700 W.

surface after the corona treatment. Therefore, depending on the corona treatment power and time, different effects can be seen at various stages. The results indicated that the surface roughness of all the

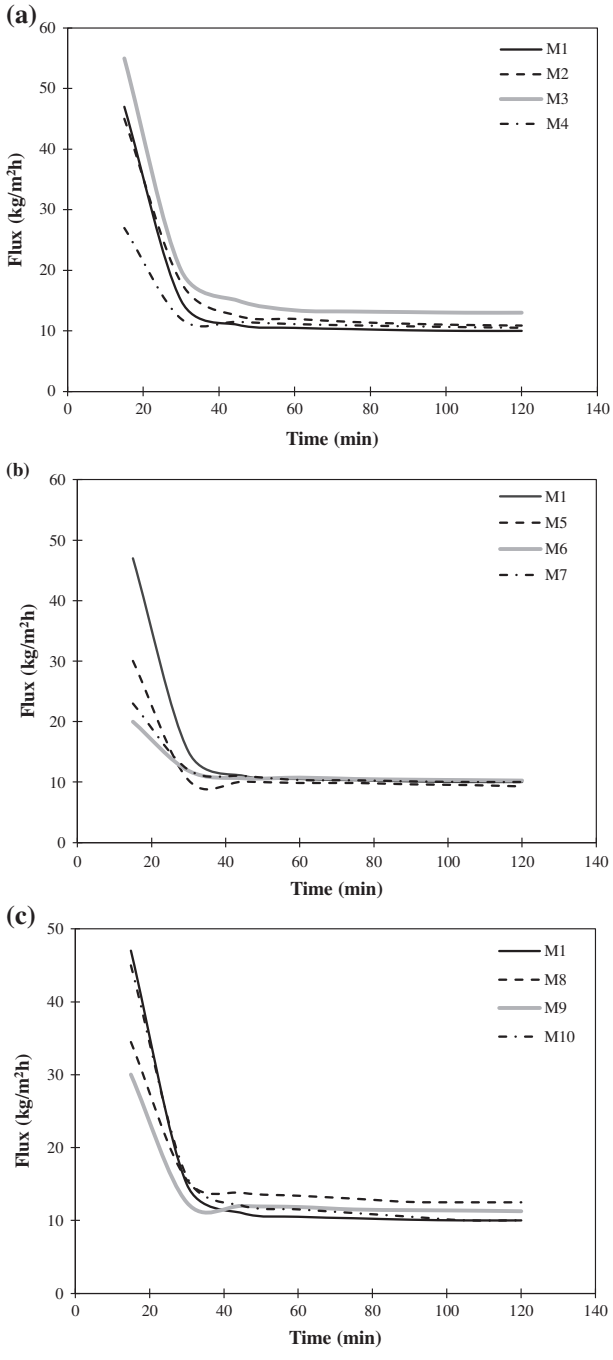

Fig. 9. The milk flux of the neat PES membrane and corona-modified membranes at different corona powers: (a) 300 W, (b) 500 W, and (c) 700 W.

corona-modified PES membrane was lower than the neat PES membrane due to the deposition of the etched materials on the membrane surface. On the other hand, the deposition of the etching materials on the membrane surface just after the etching leads to a smooth membrane surface in comparison to the neat membrane. Similar observations were reported by Sadeghi et al. [37] and Zarshenas et al. [39] which employed the corona treatment for modification of the PES and polyamide membranes, respectively. Pal et al. [46] also observed that the PES membranes have smoother surface after cold CO_2 plasma under optimal treatment conditions.

The SEM analysis was also employed to evaluate the morphology and structure of the PES membranes after the modification using the corona air plasma. Fig. 7 shows the SEM image from the surface of the neat PES membrane as well as the membrane modified by the corona treatment at different exposure times and input powers. These SEM images clearly reveal the influence of the corona treatment on the modification of the membrane surface. A comparison between the SEM image of the corona-treated membranes and the neat one indicated that the surface porosity and pore size are significantly changed and the corona modification has different effects on the morphology of the membrane surface depending on the corona treatment conditions, i.e. the corona input power and exposure time. These observations are consistent with the previous studies [37,39]. Sadeghi et al. [37] reported that the corona modification of the PES UF membranes increased the membrane pore size. Also, Zarshenas et al. [39] observed that the corona air plasma-modified membranes had a different top surface in comparison to the untreated membrane and an increase in the corona power and exposure time led to a progressive rugged surface.

Moreover, the bulk porosity and mean pore size of the neat and modified PES membranes are presented in Table 4. It was found that the porosity of the corona-modified membranes was close to that of the neat PES membrane. This implies that the surface modification of the PES membranes by the corona air plasma had no considerable effect on the bulk porosity of the membranes. However, the corona modification affected the mean pore size of the PES membranes depending on the corona applied power and exposure time. The mean pore size of all corona-treated membranes except M3 and M8 membranes decreased after the corona modification. This can be attributed to participation of the etched polymer particles on the membrane surface that decreases the surface pore size, as mentioned before. The previous studies showed that the corona modification of the PES membranes changed the pore size of the membrane depending on the corona treatment conditions [37–39]. For instance, Moghimifar et al. [38] reported that the neat PES UF membrane had lower average pore size than the modified membranes and related it to the damaging effect

Table 5
The steady state water and milk fluxes, the protein permeability, and microbe rejection of the neat and corona-treated membranes

Membrane	Water flux (kg/m^2 h)	Milk flux (kg/m^2 h)	Protein permeability (%)	Microbe rejection (%)
M1	13,600 ± 250	10.0 ± 1.3	30.4 ± 2.1	54.6 ± 4.3
M2	12,800 ± 330	10.9 ± 0.9	20.7 ± 4.2	89.9 ± 2.7
M3	16,000 ± 170	13.6 ± 1.6	32.0 ± 1.9	74.1 ± 3.3
M4	8,200 ± 210	12.0 ± 1.2	17.2 ± 3.1	92.4 ± 2.1
M5	8,900 ± 230	11.1 ± 0.9	18.5 ± 2.3	75.0 ± 4.1
M6	8,000 ± 170	11.4 ± 1.1	15.1 ± 3.2	80.3 ± 2.9
M7	11,700 ± 210	10.5 ± 1.0	23.2 ± 2.5	84.5 ± .17
M8	15,400 ± 320	12.5 ± 1.4	33.3 ± 1.4	90.3 ± 2.5
M9	7,800 ± 220	12.5 ± 1.8	17.4 ± 2.2	83.7 ± 4.0
M10	14,700 ± 190	11.8 ± 1.4	25.3 ± 1.7	89.6 ± 2.6

of the corona treatment which disrupted the upper structure of the membranes leading to a more open framework. On the other hand, Zarshenas et al. [39] observed that the prolonged corona treatment caused formation of cracks and defects on the membrane surface.

3.2. Microfiltration performance of the membrane

The separation performance of the prepared membranes was evaluated by the microfiltration experiments using pure water and skim milk as feed stream. Figs. 8 and 9 present the pure water and skim milk permeation fluxes of the neat and corona-modified PES membranes vs. time, respectively. Moreover, Table 5 gives the steady state water and milk fluxes, the protein permeability and microbe rejection of different membranes. It can be observed from Fig. 8 that for all the modified membranes, the initial pure water flux was higher than the neat one. This is due to the formation of hydrophilic functional groups on the membrane surface after the corona air plasma treatment. However, the steady state pure water flux for most of the corona-modified membranes was less than the neat PES membrane which is due to the pore size reduction of the modified membranes, as discussed in the previous section. The M3 membrane sample had the highest steady state pure water flux; since it had the bigger pore. These observations are consistent with the FTIR-ATR and SEM results. Also, the milk flux of all the modified membranes was higher than that of the neat PES membrane. The M3 membrane had the highest skim milk permeability which is due to its bigger pore size. The protein permeability values presented in Table 5 show that the M3 and M8 membrane samples had the highest protein permeability which could be attributed to their bigger pore size. The presence of the polar functional groups on the membrane surface increased the hydrophilicity of the membrane surface that reduced the deposition and accumulation of organic species like proteins on the membrane surface. Hence, the fouling propensity was lower for these membranes. However, its larger pore size also resulted in lower mass transport resistance, which facilitated the transfer of milk protein through the membrane, as can be seen by the higher protein permeability rate.

Finally, the microbial separation performance of the prepared membranes was investigated by measuring the microbial load of the feed, permeate, and retentate streams after 2 h filtration by the colony count method and the results are presented in Fig. 10. Results indicated that the microbial content of the permeate samples was decreased for all corona-treated membranes in comparison with the neat PES membrane, but due to microbial accumulation at retentate stream, its microbial content increased. Also, the microbe rejection values (Table 5) of various membranes indicated that a substantial reduction in the microbial count can be obtained by the microfiltration of milk with the corona-modified membranes. The separation mechanism in the MF process is based on the sieving effect and particles are separated solely according to the dimensions, i.e. the particle dimensions in relation to the pore size distribution of the membrane determine whether or not a particle can pass through the membrane. As presented in Table 4, most of the corona-treated PES membranes have a lower average pore size than the untreated one. Fewer microorganisms can transfer through the membranes with smaller pores which results in higher microbe rejection.

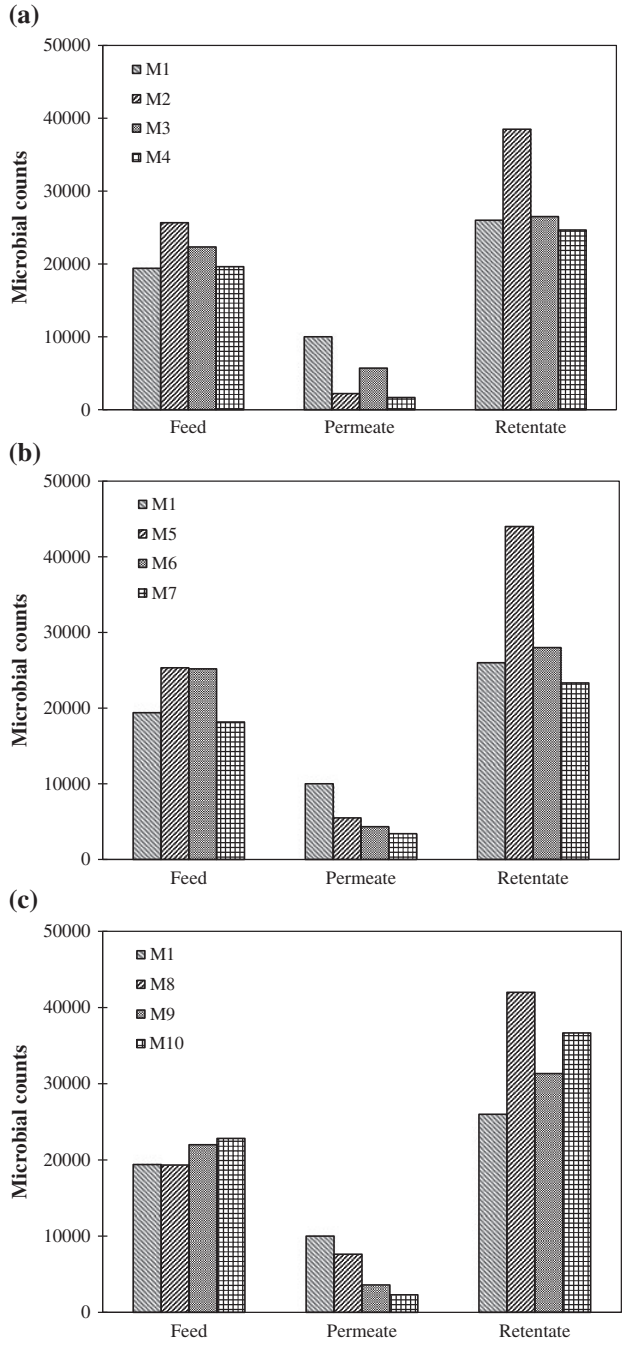

Fig. 10. The microbial content of the feed, permeate, and retentate of the milk microfiltration with the neat PES membrane and corona-modified membranes at different corona powers: (a) 300 W, (b) 500 W, and (c) 700 W.

3.3. Antifouling performance of the membrane

In order to evaluate the antifouling performance of the prepared membrane, the flux recovery as well as the mass transport resistances was calculated and the results are presented in Table 6. The flux recovery value that indicates the recycling property of the membrane, for all the corona-modified PES membranes, was higher than the neat PES membrane. Also, the cake resistance that represents the formation of a cake layer on the membrane surface due to the deposition and accumulation of the foulants on the membrane surface was the main resistance to transport and the intrinsic membrane and the fouling resistances were low for the untreated and corona-treated membranes. The fouling resistance is due to the pore plugging and the irreversible adsorption of the foulants like protein on the surface and wall of the membrane pores. It can be seen that the values of the fouling, cake, and total resistances for the corona-modified PES membranes were lower than the neat one. These results clearly imply that the antifouling performance of the PES MF membranes modified by the corona air plasma considerably improved. This behavior can be attributed to the changes in the hydrophilicity and polarity of the membranes as well as the variations in the membrane surface morphology which were induced by the corona modification. As the FTIR-ATR and contact angle analysis indicated, the membrane surface hydrophilicity and wettability of the corona-treated membranes were higher than the neat PES membrane. Therefore, the deposition and adsorption of hydrophobic components in the skim milk including proteins on the membrane surface was decreased, and consequently led to lower membrane fouling in comparison to the neat membrane. These observations agree with the common results obtained by other researchers [38,47]. Rahimpour and Madaeni [47] reported that the antifouling performance of the PES UF membranes was meliorated by incorporation of cellulose acetate phthalate (CAP) into the membrane matrix and the cake and total filtration resistance of the PES/CAP membranes were lower than the neat PES membrane. Also, Moghimifar et al. [38] observed that the PES UF membranes which were modified by the corona plasma-assisted coating TiO_2 nanoparticles had high antifouling properties and long-term flux stability in comparison to the neat PES membrane.

Finally, based on the separation performance tests and antifouling analysis of the corona-modified PES MF membranes, it was found that the M8 membrane sample had the highest FRR and protein permeability and reasonable milk flux and microbe rejection in comparison with other membrane samples. This means that the corona treatment at input power of 700 W for 7 min exposure time is the optimal condition for the modification of the PES MF membranes by the corona air plasma.

Table 6
The flux recovery and transport resistances of the neat and corona-modified membranes

Membrane	FRR (%)	R_m ($\times 10^{10}$ m^{-1})	R_f ($\times 10^{10}$ m^{-1})	R_c ($\times 10^{13}$ m^{-1})	R_t ($\times 10^{13}$ m^{-1})
M1	36.7	2.97	5.30	1.85	1.86
M2	47.9	2.30	2.50	1.75	1.75
M3	57.6	2.21	1.63	1.40	1.40
M4	39.5	2.96	4.27	1.58	1.59
M5	43.1	2.98	3.93	1.68	1.89
M6	44.8	3.44	4.24	1.67	1.68
M7	54.9	2.89	2.37	1.63	1.83
M8	86.5	3.45	2.15	1.53	1.53
M9	37.2	2.93	4.61	1.52	1.53
M10	57.8	2.42	2.88	1.61	1.62

4. Conclusions

The surface of the PES microfiltration membranes which were prepared by a combination of the vapor-induced phase inversion and nonsolvent-induced phase inversion technique were modified by the corona air plasma in order to enhance the antifouling properties and separation performance of the membranes. The influence of the corona treatment conditions including the exposure time and applied power on the surface properties of the membrane and the separation performance for reducing the microbial load of the skim milk was investigated. The results indicated that the corona air plasma modification of the PES MF membranes had significant effects on the hydrophilicity and wettability of the membrane surface as well as on the morphology and structure of the membrane surface depending on the corona treatment power and exposure time. It was observed that for all the corona-modified membranes, the initial pure water flux was higher than the neat PES membrane due to the formation of hydrophilic functional groups on the membrane surface after the corona air plasma treatment. Furthermore, the microbial analysis of the microfiltered milk revealed that a substantial reduction in the microbial count can be obtained by the microfiltration of milk with the corona-modified PES membranes. Finally, the analysis of the filtration transport resistances indicated that the cake resistance was the main resistance to transport and the fouling, cake and total resistances for the corona-modified membranes were lower than the neat one. These results imply that the antifouling performance of the PES MF membranes modified by the corona air plasma considerably improved.

References

[1] R. Baker, Membrane Technology and Applications, third ed., John Wiley & Sons Ltd., California, 2012.
[2] A.S. Jonsson, Microfiltration, ultrafiltration and diafiltration, in: S. Ramaswamy, H.J. Huang, B.V. Ramarao (Eds.), Separation and Purification Technologies in Biorefineries, John Wiley & Sons Ltd., California, 2013.
[3] A.W. Mohammad, Y.H. Teow, W.L. Ang, Y.T. Chung, D.L. Oatley-Radcliffe, N. Hilal, Nanofiltration membranes review: Recent advances and future prospects, Desalination 356 (2015) 226–254.
[4] W. Gao, H. Liang, J. Ma, M. Han, Z.L. Chen, Z.S. Han, G.B. Li, Membrane fouling control in ultrafiltration technology for drinking water production: A review, Desalination 272 (2011) 1–8.
[5] F. Meng, S.R. Chae, A. Drews, M. Kraume, H.S. Shin, F. Yang, Recent advances in membrane bioreactors (MBRs): Membrane fouling and membrane material, Water Res. 43 (2009) 1489–1512.
[6] N. Hilal, O.O. Ogunbiyi, N.J. Miles, R. Nigmatullin, Methods employed for control of fouling in MF and UF membranes: A comprehensive review, Sep. Sci. Technol. 40 (2005) 1957–2005.
[7] V. Kochkodan, N. Hilal, A comprehensive review on surface modified polymer membranes for biofouling mitigation, Desalination 356 (2015) 187–207.
[8] A.V.R. Reddy, D.J. Mohan, A. Bhattacharya, V.J. Shah, P.K. Ghosh, Surface modification of ultrafiltration membranes by preadsorption of a negatively charged polymer, J. Membr. Sci. 214 (2003) 211–221.
[9] C. Liu, Y. Yun, N. Wu, Y. Hua, C. Li, Effects of amphiphilic additive Pluronic F127 on performance of poly (ether sulfone) ultrafiltration membrane, Desalin. Water Treat. 51 (2013) 3776–3785.
[10] L.Y. Ng, A.W. Mohammad, C.P. Leo, N. Hilal, Polymeric membranes incorporated with metal/metal oxide nanoparticles: A comprehensive review, Desalination 308 (2013) 15–33.
[11] N. Nady, M.C.R. Franssen, H. Zuilhof, M.S.M. Eldin, R. Boom, K. Schroën, Modification methods for poly(arylsulfone) membranes: A mini-review focusing on surface modification, Desalination 275 (2011) 1–9.
[12] L.P. Zhu, X.X. Zhang, L. Xu, C.H. Du, B.K. Zhu, Y.Y. Xu, Improved protein-adsorption resistance of polyethersulfone membranes via surface segregation of ultrahigh molecular weight poly(styrene-alt-maleic anhydride), Colloids Surf., B 57 (2007) 189–197.

[13] Q. Shi, Y.L. Su, X. Ning, W.J. Chen, J.M. Peng, Z.Y. Jiang, Graft polymerization of methacrylic acid onto polyethersulfone for potential pH-responsive membrane materials, J. Membr. Sci. 347 (2010) 62–68.
[14] Q. Li, Q.Y. Bi, B. Zhou, X.L. Wang, Zwitterionic sulfobetaine-grafted poly(vinylidene fluoride) membrane surface with stably anti-protein-fouling performance via a two-step surface polymerization, Appl. Surf. Sci. 258 (2012) 4707–4717.
[15] L. Li, G.P. Yan, J.Y. Wu, Modification of polysulfone membranes via surface-initiated atom transfer radical polymerization and their antifouling properties, J. Appl. Polym. Sci. 111 (2009) 1942–1946.
[16] L. Li, G.P. Yan, J.Y. Wu, X.H. Yu, Q.Z. Guo, Surface-initiated atom-transfer radical polymerization from polyethersulfone membranes and their use in antifouling, E-Polym. 9 (2009) 303–312.
[17] J.E. Kilduff, S. Mattaraj, J.P. Pieracci, G. Belfort, Photochemical modification of poly(ether sulfone) and sulfonated poly(sulfone) nanofiltration membranes for control of fouling by natural organic matter, Desalination 132 (2000) 133–142.
[18] M.N.A. Seman, N. Hilal, M. Khayet, UV-photografting modification of NF membrane surface for NOM wfouling reduction, Desalin. Water Treat. 51 (2013) 4855–4861.
[19] J. Zhan, Z. Liu, B. Wang, F. Ding, Modification of a membrane surface charge by a low temperature plasma induced grafting reaction and its application to reduce membrane fouling, Sep. Sci. Technol. 39 (2004) 2977–2995.
[20] H. Guo, C. Geng, Z. Qin, C. Chen, Hydrophilic modification of HDPE microfiltration membrane by corona-induced graft polymerization, Desalin. Water Treat. 51 (2013) 3810–3813.
[21] K. Akamatsu, T. Furue, F. Han, S.I. Nakao, Plasma graft polymerization to develop low-fouling membranes grafted with poly(2-methoxyethylacrylate), Sep. Purif. Technol. 102 (2013) 157–162.
[22] I. Gancarz, G. Poźniak, M. Bryjak, W. Tylus, Modification of polysulfone membranes 5. Effect of n-butylamine and allylamine plasma, Eur. Polym. J. 38 (2002) 1937–1946.
[23] M.L. Steen, L. Hymas, E.D. Havey, N.E. Capps, D.G. Castner, E.R. Fisher, Low temperature plasma treatment of asymmetric polysulfone membranes for permanent hydrophilic surface modification, J. Membr. Sci. 188 (2001) 97–114.
[24] K.S. Kim, K.H. Lee, K. Cho, C.E. Park, Surface modification of polysulfone ultrafiltration membrane by oxygen plasma treatment, J. Membr. Sci. 199 (2002) 135–145.
[25] H.Y. Yu, L.Q. Liu, Z.Q. Tang, M.G. Yan, J.S. Gu, X.W. Wei, Surface modification of polypropylene microporous membrane to improve its antifouling characteristics in an SMBR: Air plasma treatment, J. Membr. Sci. 311 (2008) 216–224.
[26] E.S. Kim, Q. Yu, B. Deng, Plasma surface modification of nanofiltration (NF) thin-film composite (TFC) membranes to improve anti organic fouling, Appl. Surf. Sci. 257 (2011) 9863–9871.
[27] X.C. He, H.Y. Yu, Z.Q. Tang, L.Q. Liu, M.G. Yan, J.S. Gu, X.W. Wei, Reducing protein fouling of a polypropylene microporous membrane by CO_2 plasma surface modification, Desalination 244 (2009) 80–89.
[28] B. Jaleh, P. Parvin, P. Wanichapichart, A.P. Saffar, A. Reyhani, Induced super hydrophilicity due to surface modification of polypropylene membrane treated by O_2 plasma, Appl. Surf. Sci. 257 (2010) 1655–1659.
[29] R.S. Juang, C. Huang, C.L. Hsieh, Surface modification of PVDF ultrafiltration membranes by remote argon/methane gas mixture plasma for fouling reduction, J. Taiwan Inst. Chem. Eng. 45 (2014) 2176–2186.
[30] I. Yared, S.L. Wang, M.J. Wang, Effects of oxygen plasma and dopamine coating on poly(vinylidene fluoride) microfiltration membrane for the resistance to protein fouling, IEEE Trans. Plasma Sci. 42 (2014) 3847–3857.
[31] A. Lin, S. Shao, H. Li, D. Yang, Y. Kong, Preparation and characterization of a new negatively charged polytetrafluoroethylene membrane for treating oilfield wastewater, J. Membr. Sci. 371 (2011) 286–292.
[32] X. Wei, B. Zhao, X.M. Li, Z. Wang, B.Q. He, T. He, B. Jiang, CF_4 plasma surface modification of asymmetric hydrophilic polyethersulfone membranes for direct contact membrane distillation, J. Membr. Sci. 407–408 (2012) 164–175.
[33] M. Bryjak, I. Gancarz, G. Poźniak, W. Tylus, Modification of polysulfone membranes 4. Ammonia plasma treatment, Eur. Polym. J. 38 (2002) 717–726.
[34] F. Dreux, S. Marais, F. Poncin-Epaillard, M. Metayer, M. Labbe, Surface modification by low-pressure plasma of polyamide 12 (PA12). Improvement of the water barrier properties, Langmuir 18 (2002) 10411–10420.
[35] A. Batsch, D. Tyszler, A. Brügger, S. Panglisch, T. Melin, Foulant analysis of modified and unmodified membranes for water and wastewater treatment with LC-OCD, Desalination 178 (2005) 63–72.
[36] D. Tyszler, R.G. Zytner, A. Batsch, A. Brügger, S. Geissler, H. Zhou, D. Klee, T. Melin, Reduced fouling tendencies of ultrafiltration membranes in wastewater treatment by plasma modification, Desalination 189 (2006) 119–129.
[37] I. Sadeghi, A. Aroujalian, A. Raisi, B. Dabir, M. Fathizadeh, Surface modification of polyethersulfone ultrafiltration membranes by corona air plasma for separation of oil/water emulsions, J. Membr. Sci. 430 (2013) 24–36.
[38] V. Moghimifar, A. Raisi, A. Aroujalian, Surface modification of polyethersulfone ultrafiltration membranes by corona plasma-assisted coating TiO_2 nanoparticles, J. Membr. Sci. 461 (2014) 69–80.
[39] K. Zarshenas, A. Raisi, A. Aroujalian, Surface modification of polyamide composite membranes by corona air plasma for gas separation applications, RSC Adv. 5 (2015) 19760–19772.
[40] B. Jiang, J.Z.S. Zheng, S. Qiu, M. Wu, Q. Zhang, Review on electrical discharge plasma technology for wastewater remediation, Chem. Eng. J. 236 (2014) 348–368.
[41] H. Susanto, N. Stahra, M. Ulbricht, High performance polyethersulfone microfiltration membranes having high flux and stable hydrophilic property, J. Membr. Sci. 342 (2009) 153–164.

[42] M. Toroghi, A. Raisi, A. Aroujalian, Preparation and characterization of polyethersulfone/silver nanocomposite ultrafiltration membrane for antibacterial applications, Polym. Adv. Technol. 25 (2014) 711–722.
[43] G.T. Pyne, The determination of milk-proteins by formaldehyde titration, Biochem. J. 26 (1932) 1006–1014.
[44] C. Güell, R.H. Davis, Membrane fouling during microfiltration of protein mixtures, J. Membr. Sci. 119 (1996) 269–284.
[45] J.F. Li, Z.L. Xu, H. Yang, C.P. Feng, J.H. Shi, Hydrophilic microporous PES membranes prepared by PES/PEG/DMAc casting solutions, J. Appl. Polym. Sci. 107 (2008) 4100–4108.
[46] S. Pal, S.K. Ghatak, S. De, S. DasGupta, Evaluation of surface roughness of a plasma treated polymeric membrane by wavelet analysis and quantification of its enhanced performance, Appl. Surf. Sci. 255 (2008) 2504–2511.
[47] A. Rahimpour, S.S. Madaeni, Polyethersulfone (PES)/cellulose acetate phthalate (CAP) blend ultrafiltration membranes: Preparation, morphology, performance and antifouling properties, J. Membr. Sci. 305 (2007) 299–312.